Determination of the antibacterial, antioxidant and photocatalytic activity of AgNPs green synthesized using extracts of 5 species of the *Diospyros* genus.

Venuja Jayawardena[1] and Mathivathani Kandiah[1*]

[1]School of Science, Business Management School (BMS), Sri Lanka

*mathi@bms.ac.lk

Abstract

The use of nanoparticles in various industries have increased over the years with the improvement of the methods of nanoparticle synthesis which uses less energy at a cheaper cost through the use of eco-friendly materials such as plants and microorganisms. Silver nanoparticles (AgNPs) were synthesized in an eco-friendly method using six species of *Diospyros* leaf extracts under various temperature conditions where the optimum conditions were at a temperature of 90 °C for an hour. All species of *Diospyros* produced spherical AgNPs, with the exception of *Diospyros malabarica*, of an average diameter of 30 nm when viewed under TEM. These AgNPs were classified as semiconductors once the bandgap energy was calculated with a surface plasmon resonance at a wavelength of 420 nm. The AgNPs and the water extracts were tested for their antioxidant capabilities through Total antioxidant Capacity (TAC), Total Flavonoid Content (TFC), Total Phenolic Content (TPC), DPPH and IC_{50} assays which revealed that the AgNPs had better antioxidant activity than the water extracts with *Diospyros oocarpa* having the highest activity. The photocatalytic activity of different concentrations of the AgNPs were measured by measuring the degradation of the organic dye, Eriochrome Black T where 333 ppm AgNPs had the highest degradation rate with the use of $NaBH_4$. In addition, the antibacterial activity of the AgNPs and water extracts was measured and compared against *Staphylococcus aureus* and *Escherichia coli*, where the AgNPs had greater antibacterial activity against *Staphylococcus aureus* due to higher greater zones of inhibition. The properties of *Diospyros* AgNPs were determined and the possible uses the AgNPs can be used in several industries.

Keywords: *Diospyros*, silver, nanoparticles, antioxidant, antibacterial, photocatalytic

1. Introduction

Nanoscience is classified as the field of study of nano-structures, where nanotechnology utilises nanoscience into various applications through the manipulation of nanoparticles, that are structures of at least one dimension of length ranging from 1 to 100 nanometres.[1,2] Different nanoparticles are of different sizes and compositions ranging from liposomes and micelles to quantum dots and metallic nanoparticles.[3]

Metallic nanoparticles of various metals of gold, silver, copper, platinum and palladium, are used routinely in several applications ranging from biomedical to environmental applications.[4,5] Several properties of AgNPs such as the large surface area to volume ratio, surface plasmon resonance and the strong antimicrobial ability led to the employment of these nanoparticles in applications such as drug delivery, cell imaging, wastewater treatment, UV protection and photocatalysis,[6-9]

AgNPs are used as antibacterial agents as these nanoparticles are known to exert bactericidal action through various mechanisms by the release of silver ions, resulting in the significant inhibition of the growth of bacteria as illustrated in Figure 1.[10, 11]
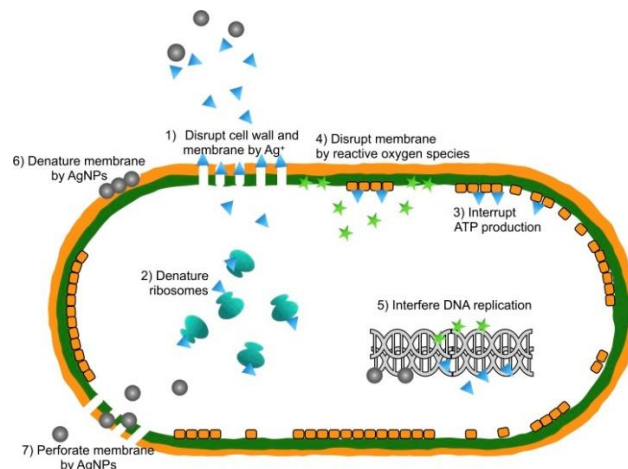

Figure 1. The antibacterial mechanisms of AgNPs.[12]

Other applications of AgNPs such as hydrogen production from wastewater and dye effluent treatment are carried out through photocatalysis. Photocatalysis is the ability of the particle to undergo oxidation when exposed to UV light, creating electron-hole pairs when an excited electron transitions from the valence band to the conduction band, forming free radicals which breakdown organic compounds as shown in Figure 2.[13,14]
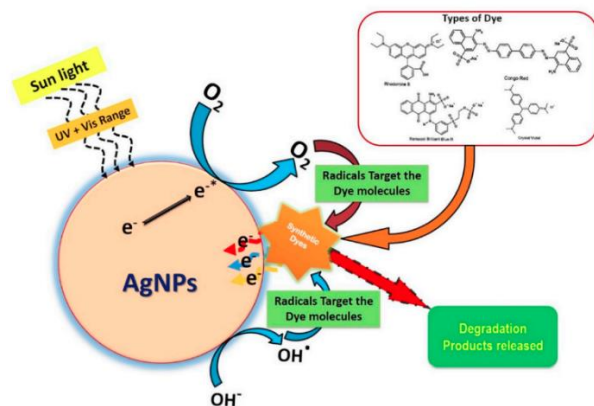
Figure 2. Photocatalytic degradation of an organic compound.[13]

In addition, AgNPs are known to be used in the treatment of cancer due to their antioxidant properties.[15] Antioxidants are compounds that inhibit oxidation reactions, preventing the formation of free radicals which cause oxidative stress (Figure 3).[16] The antioxidants in plant extracts primarily consist of flavonoids and phenols.[17, 18]
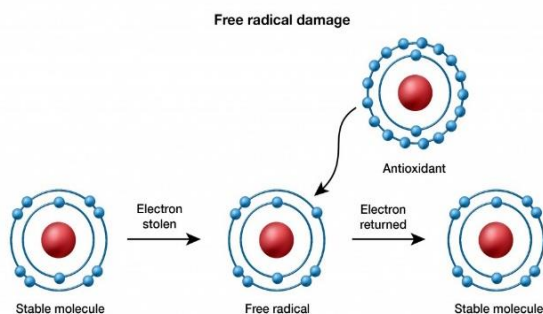

Figure 3. Mechanism of action of antioxidants.[18]

Oxidative stress in the human body can be defined as the imbalance between the number of free radicals, which is an atom with an unpaired electron, and the number of antioxidants, causing tissue damage due to the elevated levels of reactive oxygen species (ROS).[19,20] These high levels of ROS can be caused by the exogenous factors such as radioactivity and endogenous factors such as deficiencies in antioxidant enzymes, leading to harmful conditions such as macular degeneration, cardiac fibrosis, skin aging and auto-immune disorders.[21,22]

Oxidative stress is prevented in the body by antioxidants, which are primarily supplied through dietary sources such as citrus fruits.[23] AgNPs which show significant antioxidant activity can be utilized to decrease the concentration of ROS, reducing oxidative stress such as the

loading of nanoparticles into hydrogels to prevent skin aging.[24]
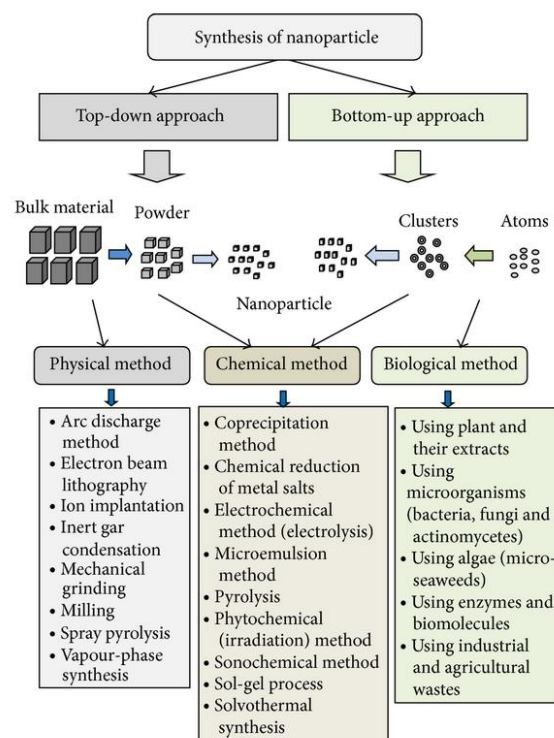
Figure 4. Approaches to the synthesis of nanoparticles.[27]

Table 1. Advantages and disadvantages of the approaches to the synthesis of nanoparticles.[30, 31]

|	Advantages	Disadvantages
Top-Down	• Large scale production • Requires no purification	• Relatively expensive • Size distribution
Bottom-Up	• Relatively cheap • Able to control size and shape of nanoparticles	• Cannot be employed for large scale production

The approaches to the synthesis of nanoparticles can be divided into the Top-Down and the Bottom-Up approach (Figure 4), with their individual advantages and disadvantages (Table 1).[25, 26] The Top-Down approach involves the breakdown of large bulk material into smaller particles through physical or chemical methods until particles of the nanoscale are reached.[27, 28] Bottom-Up approach involves the build-up of nanoparticles using simpler particles such as atoms and molecules through chemical and biological methods.[27, 29] The physical synthesis of nanoparticles involves the breaking of larger materials through processes such as grinding and evaporation which require large quantities of energy and space, while being

time-consuming.[30] Chemical processes primarily use chemicals acting as reducing agents which synthesizes nanoparticles through the reduction of metallic ions, at the risk of chemical contamination.[31]
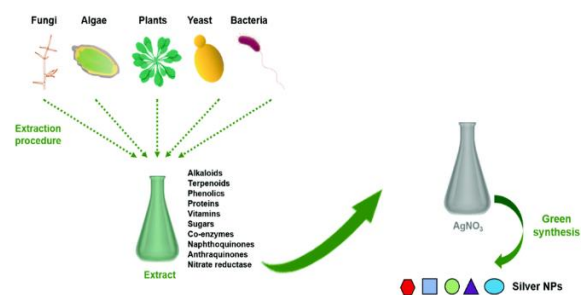

Figure 5. Green synthesis of AgNPs.[33]

The biological synthesis (green synthesis) of nanoparticles employs the use of biodegradable materials, such as plants and microbial organism, for the synthesis of metallic nanoparticles from their ionic form (Figure 5).[32, 33] In this study, leaves were preferred as a raw material due to the ease in obtaining the leaf extract, low cost and abundance in raw materials whereas microorganisms require constant culture maintenance.[34]
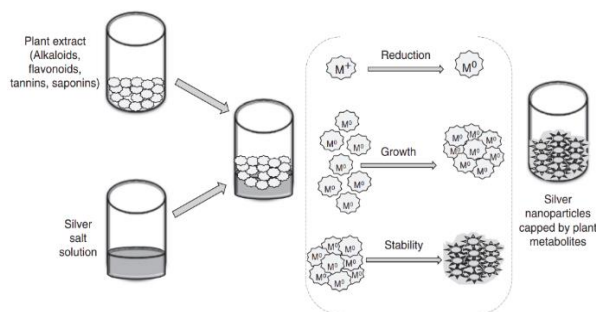
Figure 6. Formation of metallic nanoparticles.[35]

The mechanism through which metallic nanoparticles form (Figure 6) involve the mixing of the plant extracts in a metal-salt solution under certain conditions which results in the reduction of metal ions (M^+) to their metallic form (M^0), leading to nucleation, growth and stabilization of the nanoparticles.[35] Phytochemicals such as flavonoids and phenols, in the plant extracts act as reducing and stabilizing agents in nanoparticle synthesis.[36]

The green synthesis is more favourable due to the cost-effectiveness, the availability of samples, environmental friendliness, disuse of toxic chemicals and compounds, and the ability to manipulate the size and shape of the nanoparticles.[37,38]
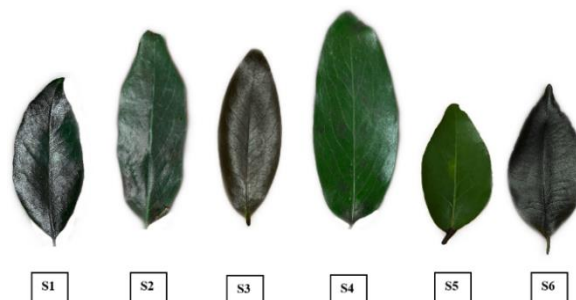
Diospyros affinis	S1
Diospyros atrata	S2
Diospyros ebenum	S3
Diospyros malabarica	S4
Diospyros oocarpa	S5
Diospyros quaesita	S6

Figure 07. Species of *Diospyros* used

The leaf samples used in this study are of the species, *Diospyros*, from the Ebenaceae family, and is a genus of over 500 species of plants and shrubs which are distributed pantropically around the world.[39] The species of *Diospyros* used in this study are outlined in Figure 7.

Different parts of the *Diospyros* species have been used in several industries where fruit-yielding species include *D. kaki, D. lotus* and *D. virginiana,* whereas species such as *D. ebenum* and *D. celebica* are used for their timber.[40] In addition, a number of species are used for therapeutic purposes in traditional medicine to treat conditions such as hypertension, atherosclerosis, asthma and infectious diseases.[41, 42]

These samples were selected for this study as previous studies have concluded that titanium and selenium nanoparticles, synthesized using leaf extracts from species of *Diospyros*, possess significant antibacterial properties against gram-positive bacteria and significant antioxidant activity.[43,44]

Hence assessing the properties of AgNPs synthesized from leaf extracts of *Diospyros*, determines for which applications these nanoparticles can be used for.

The aim of this study is to synthesize AgNPs from leaf extracts of the six species of *Diospyro*s through green synthesis. The antioxidant activity of the extracts will be measured through TAC, TFC, TPC, DPPH and IC_{50} assay, whereas the antibacterial activity will be assessed using the well diffusion method with bacterial strains of *Staphylococcus aureus* and *Escherichia coli.* The photocatalytic activity of the nanoparticles will be measured through the degradation of organic dyes, and the presence of phytochemicals will be confirmed through various assays.

2. Methodology

Good laboratory practice was maintained when carrying out nanoparticle synthesis and the relevant assays to determine its properties and the relevant COOSH forms were filled out when requesting the required chemical reagents.

2.1 Sample collection. Leaves from six species of the *Diospyros* genus (Figure 7) were selected and collected from the Royal Botanic Garden in Peradeniya, Sri Lanka. The samples can be identified using the below key (Table 2).

Table 2: Sample key

Species of *Diospyros*	Code
Diospyros affinis	S01
Diospyros atrata	S02
Diospyros ebenum	S03
Diospyros malabarica	S04
Diospyros oocarpa	S05
Diospyros quaesita	S06

2.2. Preparation of leaf extracts. The leaves were air-dried in the shade for 72 hours and ground into a fine powder, from which 2 g of each sample was mixed with 50 ml of distilled water. The samples were placed in the dry oven for 15 minutes at 85 °C and filtered into a 50 ml Falcon tube using a Whatman No. 1 filter paper. The prepared leaf extracts were placed in the 4 ^{0}C for future use.

2.3. Phytochemical analysis. The presence of the below phytochemicals in the leaf extracts of *Diospyro*s was confirmed using the below tests (Table 3).

Table 3. Methodology to confirm the presence of phytochemicals

Phytochemical	Methodology	Positive Result
Anthraquinones	4 - 5 drops of 10% ammonium hydroxide solution were added to 1 ml of the leaf extract.[45]	A pink colour precipitate will be formed.
Carbohydrates	1 ml of the Molisch's reagent was added to 2 ml of the plant extract along with 4 - 5 drops of concentrated sulfuric acid.[46]	A reddish-purple ring will be formed.
Proteins	A few drops of copper sulfate were added into the leaf extract along with 1 ml of 10% sodium hydroxide.[47]	A dark bluish-purple colour will be formed.
Saponins	0.2 g of the dried leaf extract was shaken with 5 ml of distilled water. The solution was heated to boiling.[45]	
Steroids	1 ml of chloroform was added into 1 ml of the leaf extract along with a few drops of concentrated sulfuric acid.[47]	A brown colour ring will be formed.
Tannins	3 ml of 5% Iron Chloride was added into 1 ml of the leaf extract.[45]	A dark green-blue colour will be formed.
Terpenoids	2 ml of chloroform was added into 0.5 ml of the leaf extract along with a few drops of concentrated sulfuric acid.[45]	A reddish – brown colour will be formed at the interface.

2.3. Synthesis of AgNPs. 9 ml of 1 mM solution of Silver nitrate was mixed with 1 ml of the leaf extracts, and placed in the dry oven for 1 hour at 90 °C. The absorbance of the samples was measured at wavelengths ranging from 320 nm to 520 nm using distilled water as the blank.

2.3.1 Optimisation of AgNP synthesis. 9 ml of 1 mM solution of Silver nitrate was mixed with 1 ml of the leaf extracts and placed in the incubator at different temperatures for different periods of time which include 30 minutes at 90 °C, 1 hour at 60 °C, 30 minutes at 90 °C and 72 hours at 25 °C (Room Temperature). The absorbance of the samples was measured at wavelengths from 320 nm to 520 nm using distilled water as the blank.

2.4 Dilution of water extracts and AgNPs. The water extracts and the synthesised AgNPs were diluted into a 1:15 ratio using distilled water. The prepared leaf extracts were placed in the 4 °C for future use.

2.5. Antioxidant Assays. The diluted samples were used to assess the following assays.

2.5.1. Determination of the Total Flavonoid Content (TFC). A modified colorimetric method was carried out to determine the TFC using aluminium chloride.[48] A 1.2% aluminium chloride solution was prepared along with a 120 mM solution of potassium acetate. 1 ml of the sample was mixed with 0.5 ml of the 1.2% aluminium chloride and 120 mM potassium and left for 30 minutes at room temperature. The absorbance was measured in triplicates at 415 nm, using distilled water as the blank and the TFC was expressed as quercetin equivalents (QE).

2.5.2. Determination of the Total Phenol Content (TPC). The total content of phenols was determined through the Folin-Ciocalteu reagent test (48). A 20 N solution of Folin-Ciocalteu was diluted to a 1 N Folin-Ciocalteu solution using distilled water. 1 ml of the sample was mixed with 0.1 ml of the 1 N Folin-Ciocalteu reagent and were left for 15 minutes

at room temperature, and to which 5 ml of the saturated sodium carbonate solution was added. The test tubes were left for 30 minutes at room temperature and the absorbance was measured in triplicates at 760 nm, using distilled water as the blank and the TPC was expressed as gallic acid equivalents (GAE). [48]

2.5.3. Determination of the Total Antioxidant Capacity (TAC). The TAC was determined using the phosphomolybdenum assay derived from other studies.[49] The phosphomolybdenum reagent was prepared by mixing equal volumes of 0.6 M sulphuric acid, 28 mM sodium phosphate and 4 mM ammonium molybdate. 2 ml of the phosphomolybdenum reagent was mixed with 0.2 ml of the sample, and incubated for 90 minutes at 95 °C. The absorbance was measured in triplicates at 695nm, using distilled water as the blank and the TAC was expressed as ascorbic acid equivalents (AAE). [48]

2.5.4. Determination of the DPPH scavenging activity. 0.004% of the DPPH solution was prepared by mixing 0.0054 g of DPPH in 100 ml of methanol to which 1 ml of the sample was added to 1 ml of DPPH solution. The samples were incubated for 30 minutes and the absorbance was measured at 517 nm, using methanol as the blank. The DPPH scavenging activity was calculated using the below equation.

$$\text{DPPH Percentage Scavenging Activity}$$

$$= \frac{\%\ \text{Activity}_{\text{Control}} - \%\ \text{Activity}_{\text{Sample}}}{\%\ \text{Activity}_{\text{Control}}} \times 100$$

2.5.5. Determination of the Median Inhibition Concentration (IC$_{50}$). 0.004% of the DPPH solution was prepared by mixing 0.0054 g of DPPH in 100 ml of methanol. A 100%, 80%, 60%, 40% and 20% solutions were prepared using the samples and distilled water to which 2 ml of the 0.004% DPPH solution was added. The solutions were incubated for 30 minutes at room temperature and the absorbance was measured at 517 nm, using methanol as the blank. The percentage activity was calculated using the above equation and the IC$_{50}$ was determined.

2.6. Determination of the Photocatalytic Activity. A 2 mM solution of Eriochrome Black T (EBT) was prepared to which 1 ml of the 333 ppm AgNPs was pipetted in. The absorbance of the solution was measured at a wavelength range from 320 nm to 720 nm. The solution was placed in sunlight and the absorbance was measured at 30-minute intervals, using distilled water as the blank. The experiment was also carried out after adding 1 ml of 0.2 M solution of sodium borohydride which acts as a catalyst. The experiment once again was repeated using the 5000 ppm solutions of the AgNPs.

2.7. Determination of the antibacterial activity. The antibacterial activity of the samples was determined through the well diffusion method using bacterial strains of *Staphylococcus aureus* and *Escherichia* coli. The agar plates were produced by pouring 20 ml of Mueller-Hinton agar into each plate and left to cool. Once cooled, the plates were labelled and placed under UV light for sterilisation. The plates were separately swabbed with the bacterial strains and three wells were created on the agar for the negative control (-) and two duplicates of the sample (S1 and S2) as shown in Figure 08. The positive control (+) used was a gentamycin disc, which was placed on the agar along with 0.5 mL of saline water as the negative control (-). 0.5 mL of the sample was transferred into S1 and S2, and the plates were placed in the incubator at 37 °C for 24 hours (Figure 8). Once incubated, a ruler was used to measure the diameter of the zones of inhibition.
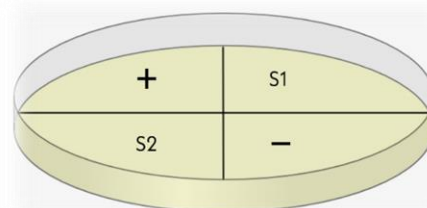
Figure 8: Labelling of agar plates

2.8. Transmission Electron Microscopy. 1 ml of the S05 AgNPs was transferred into an Eppendorf tube and centrifuged at 5000 rpm for five minutes. Once centrifuged, the Eppendorf tube was transferred into the dry oven for 48 hours. The morphology of the nanoparticles was examined at the Sri Lanka Institute of Nanotechnology using the JEM-2100 Transmission Electron Microscope.

2.9 Statistical Analysis. The statistical software, SPSS Version 25 (Statistical Package for the Social Sciences) was used to carry out the one-way ANOVA statistical test to determine a significant difference between the TFC, TPC and TAC of the water extracts and AgNPs, and the antibacterial activity of the samples against *Staphylococcus aureus* and *Escherichia coli.*

3. Results

The results of the phytochemical tests carried out on the water extracts of *Diospyros* are outlines in Table 4. Saponin is present in all the samples except in SO4. The formation of AgNPs in the extracts is indicated by the colour change from colourless to a reddish-brown solution as illustrated in Figure 9, where S01, S02, S03, S05 and S06 exhibited a colour change.
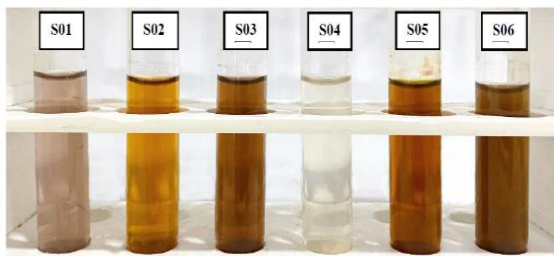
Table 4. Results of the phytochemical tests

| Phytochemical	S01	S02	S03	S04	S05	S06	Positive Result
Anthraquinones	✗	✗	✗	✗	✗	✗	-
Carbohydrates	✗	✗	✗	✓	✓	✓	
Proteins	✗	✓	✓	✗	✓	✓	
Saponins	✓	✓	✓	✗	✓	✓	
Steroids	✗	✗	✗	✗	✗	✗	-
Tannins	✗	✗	✗	✗	✗	✗	-
Terpenoids	✗	✓	✗	✗	✓	✓	

(A)
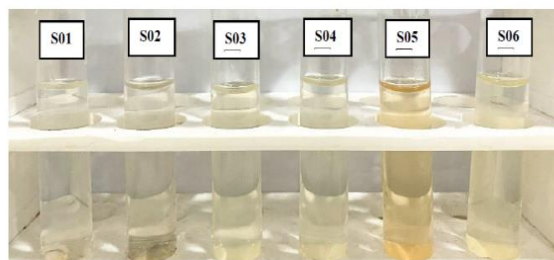
(B)

Figure 9. Colour change observed when nanoparticles are synthesized at 90 °C at 1 hour (A – Before, B – After).

The absorbance of the solutions was measured at a wavelength range from 320 nm to 520 nm, where peaks in absorbance at 420 nm indicate the formation of AgNPs (Figure 13). All the samples with the exception of S04 produced peaks at 420 nm, indicating the formation of AgNPs.
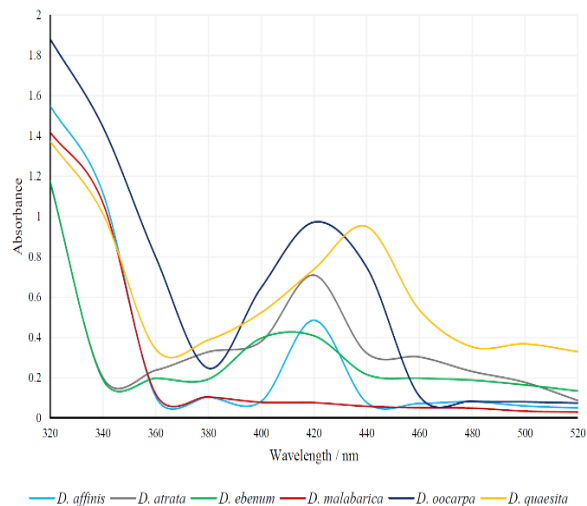
**Figure 10.** Visible spectrum for the optimized AgNPs synthesized at 90 °C at 1 hour.

Synthesis of AgNPs were carried out at temperatures of 90 °C ,60 °C and 25 °C (room temperature) for different periods of time where the optimum conditions were found to be 90 °C for 1 hour (Table 5).

Table 05. Conditions at which AgNPs were synthesized

Species of *Diospyros*	Conditions				
	25 °C (Room Temperature)	60 °C		90 °C	
	72 hours	30 minutes	60 minutes	30 minutes	60 minutes
S01	✓	✓	✗	✓	✓
S02	✓	✓	✓	✓	✓
S03	✓	✓	✓	✓	✓
S04	✗	✗	✗	✗	✗
S05	✓	✓	✓	✓	✓
S06	✓	✓	✓	✓	✓

When measuring the absorbance at wavelengths from 320 nm to 520 nm, the samples that had a peak at 400 nm to 440 nm are labelled with a ✓, indicating the presence of AgNPs.

Transmission Electron Microscopy was caried out to determine the morphology and size of the synthesized AgNPs. As illustrated on Figure 11, the AgNPs are spherical in shape with an estimated average diameter of 30 nm, ranging from 20 nm to 40 nm.
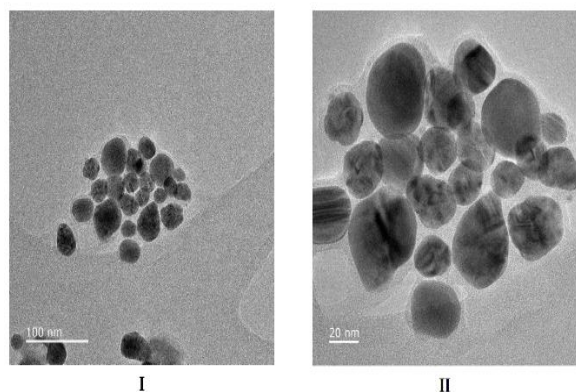
Figure 11. TEM imaging of AgNPs. I and II are in different scales.

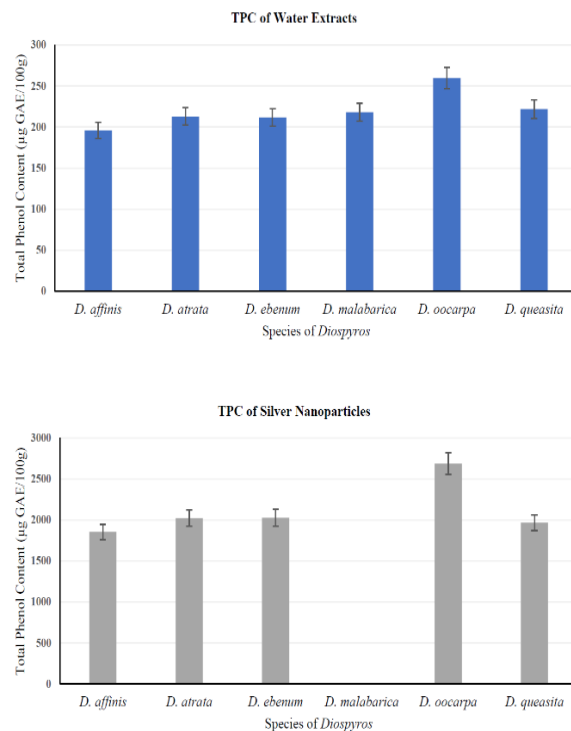*3.1. Determination of the Total Flavonoid Content*
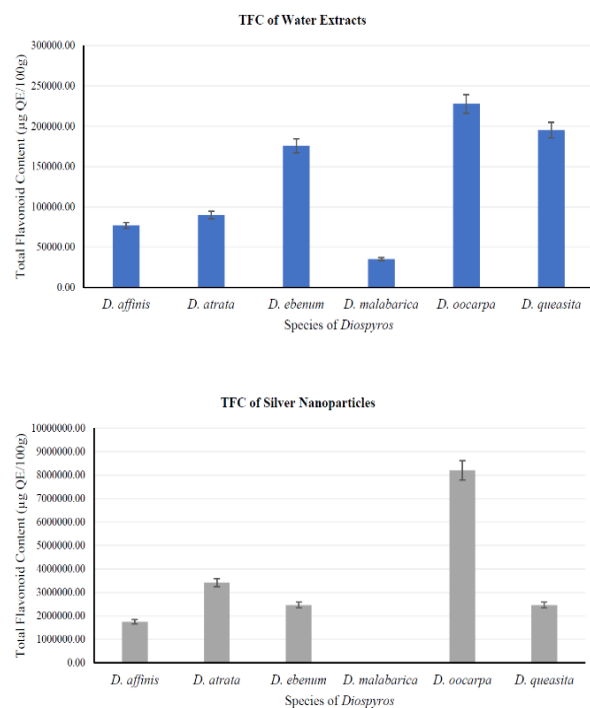
Figure 12. Total flavonoid content of water extracts and AgNPs (µg QE/100g)

As illustrated in Figure 12, the AgNPs had a higher total flavonoid content than the water extracts.

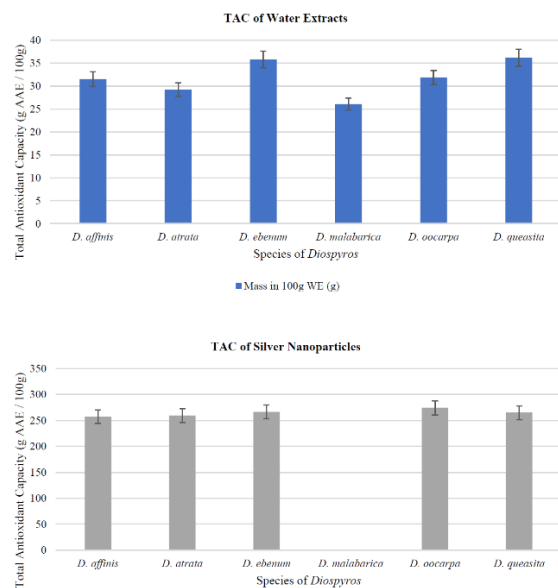*3.2. Determination of the Total Phenol Content.*

As illustrated in Figure 13, the AgNPs had a higher total phenol content than the water extracts.

Figure 13. Total phenol content of water extracts and AgNPs (µg GAE/100g)

3.3. Determination of the Total Antioxidant Capacity.

Figure 14. Total antioxidant capacity of water extracts and AgNPs (g AAE/100 g)

As illustrated in Figure 14, the AgNPs gave a higher total antioxidant capacity than the water extracts.

3.4 Statistical Analysis of TFC, TPC and TAC.

The statistical test, One-Way ANOVA was carried out to determine if there are any significant differences between the TFC, TPC and TAC of the water extracts and the AgNPs (Table 6, Table 7 and Table 8).

Table 6. One-Way ANOVA between the TFC of water extracts and AgNPs

| ANOVA						
Source of Variation	SS	df	MS	F	P-value	F crit
Between Groups	5423292.68	1	5423292.68	11.187367	0.008595	5.117355
Within Groups	4362924.127	9	484769.3474			
Total	9786216.807	10				

Table 7. One-Way ANOVA between the TPC of water extracts and AgNPs

ANOVA						
Source of Variation	SS	df	MS	F	P-value	F crit
Between Groups	1560953.065	1	1560953.065	201.47957	1.82E-07	5.117355
Within Groups	69727.05701	9	7747.450779			
Total	1630680.122	10				

Table 8. One-Way ANOVA between the TAC of water extracts and AgNPs

ANOVA						
Source of Variation	SS	df	MS	F	P-value	F crit
Between Groups	17070.56333	1	17070.56333	18.230835	0.0016376	4.9646027
Within Groups	9363.56646	10	936.356646			
Total	26434.12979	11				

3.5. Determination of the DPPH Radical Scavenging Activity.
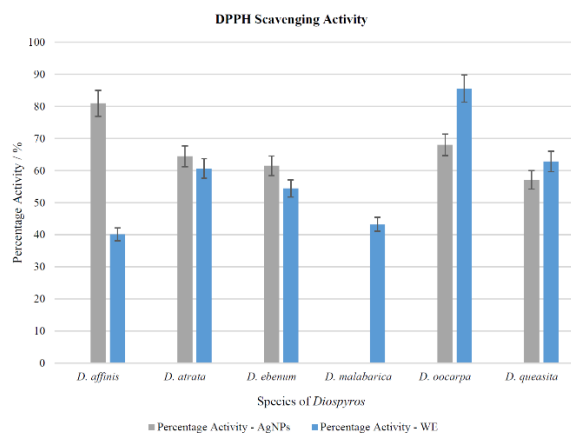
Figure 15. DPPH scavenging percentage activity of water extracts and AgNPs

The AgNPs synthesized from S01, S02 and S03 gave a higher DPPH radical scavenging percentage activity compared to the water extracts (Figure 15).

3.6. Determination of the Inhibitory Concentration (IC50) of DPPH.
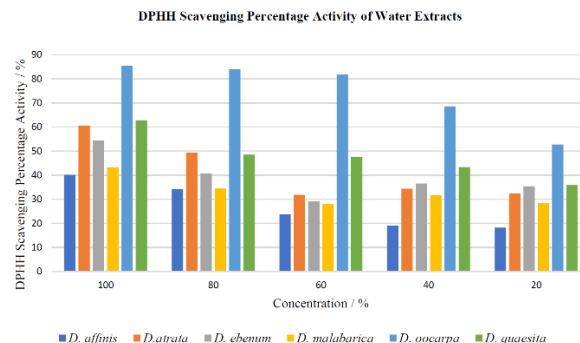
Figure 16. IC$_{50}$ of water extracts
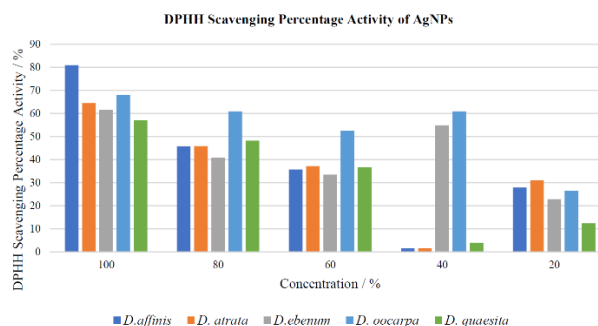
Figure 17. IC$_{50}$ of AgNPs

Table 9. IC$_{50}$ of the water extracts and the AgNPs.

Sample	IC50	
	WE	AgNPs
S01	137.69322	57.451875
S02	83.149342	85.155247
S03	110.91513	83.021492
S04	163.32515	-
S05	2.1448999	50.882992
S06	67.92998	62.255501

The IC50 values calculated for the water extracts of S01, S03 and S06 are greater than the IC50 values of the AgNPs whereas the IC50 values calculated for the water extracts of S02 and S05 are less than the IC50 values of the AgNPs.

3.7. Determination of the Photocatalytic Activity.
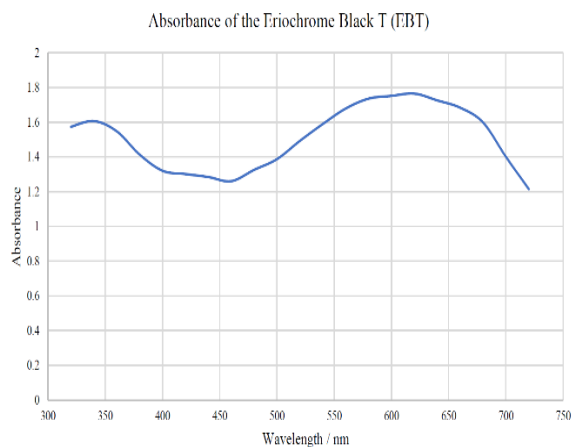
Figure 18. Absorbance of EBT from 320 nm to 720 nm

Figure 18 outlines the absorbance of EBT at wavelengths ranging from 320 nm to 720 nm, which can be used to compare the degradation of the dye by AgNPs.
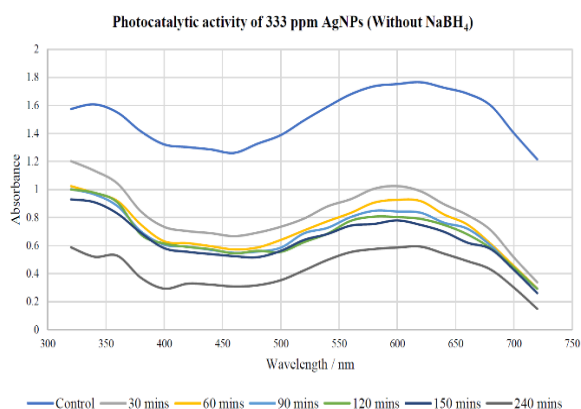
Figure 19. Photocatalytic activity of 333 ppm AgNPs (Without NaBH$_4$)

The absorbance of the dye was measured at 30-minute intervals till 150 minutes, and once again measured at the 4-hour mark (240 minutes) (Figure 19). The photocatalytic degradation rate constant was calculated to be 0.0025, using an ln (Ct/C0) against reaction time graph
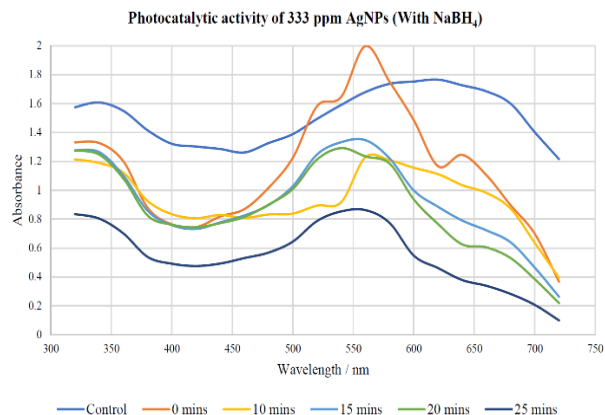
Figure 20. Photocatalytic activity of 333 ppm AgNPs (With NaBH$_4$)

The absorbance of the dye was measured at 10-minute intervals till 10 minutes, and then to 25 minutes in 5-minute intervals (Figure 20). The photocatalytic degradation rate constant was calculated to be 0.0271, using an ln (Ct/C0) against reaction time graph.
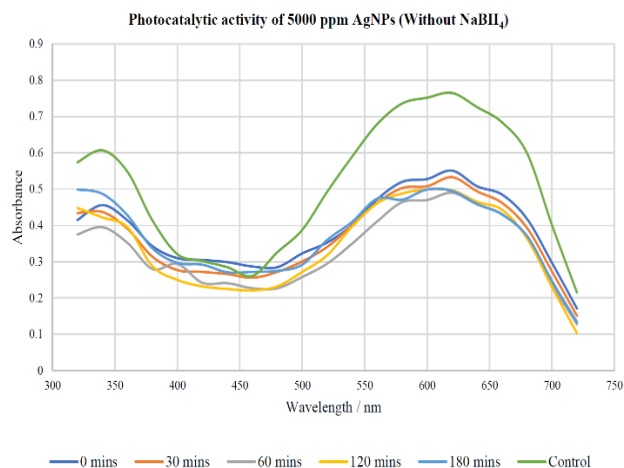
Figure 21. Photocatalytic activity of 5000 ppm AgNPs (Without NaBH$_4$)

The absorbance of the dye was measured at 30-minute intervals till 60 minutes, and then to 180 minutes in 60-minute intervals (Figure 21). The photocatalytic degradation rate constant was calculated to be 0.0005, using an ln (Ct/C0) against reaction time graph.

Figure 22. Photocatalytic activity of 5000 ppm AgNPs (With NaBH$_4$)

The absorbance of the dye was measured at 10-minute intervals till 40 minutes (Figure 22). The photocatalytic degradation rate constant was calculated to be 0.0111, using an ln (Ct/C0) against reaction time graph.

3.8 Determination of the Antibacterial Activity.

Figure 23. Antibacterial activity of the samples. (A – S04 water extract, B – S02 silver nanoparticles)

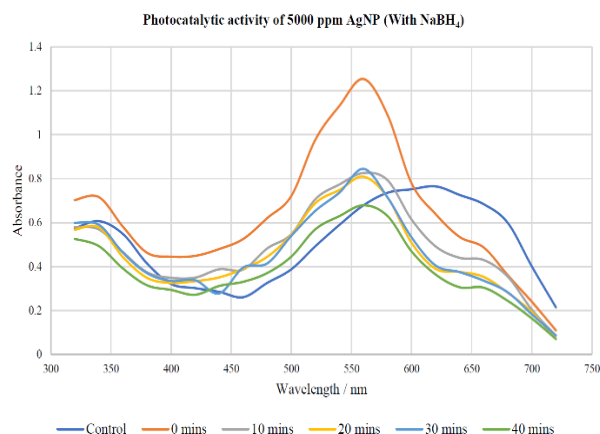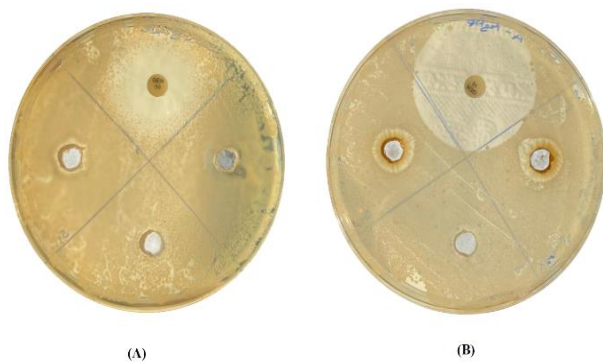The agar plates exhibited zones of inhibition (ZOI) around the samples after being incubated for 24 hours as illustrated on Figure 23.

Figure 24 and 25 compares the zones of inhibition between the water extracts and the AgNPs concluding that the AgNPs exhibit are significantly higher ZOIs than that of the water extracts against both *Staphylococcus aureus* and *Escherichia coli.*
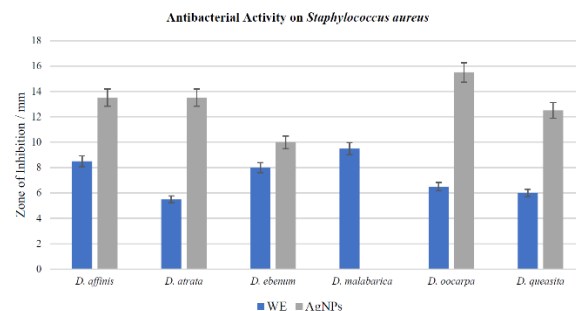
Figure 24. Antibacterial activity on *Staphylococcus aureus*
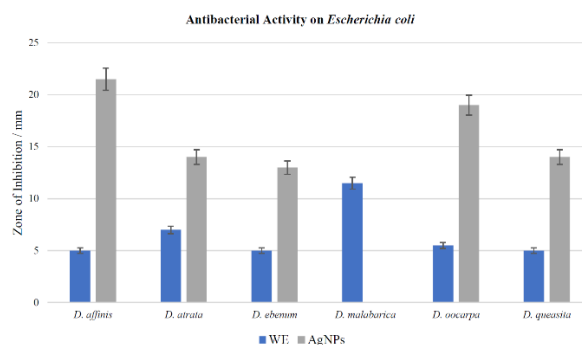
Figure 25. Antibacterial activity on *Escherichia coli*

The statistical test, One-Way ANOVA was carried out to determine if there is a significant difference between the antibacterial activity of the water extracts and the AgNPs against *Staphylococcus aureus* and *Escherichia coli* (Table 10 and Table 11).

Table 10. One-Way ANOVA between the antibacterial activity against *Staphylococcus aureus* between water extracts and AgNPs

ANOVA						
Source of Variation	SS	df	MS	F	P-value	F crit
Between Groups	87.57575758	1	87.57575758	27.818182	0.000511	5.117355
Within Groups	28.33333333	9	3.148148148			
Total	115.9090909	10				

Table 11. One-Way ANOVA between the antibacterial activity against *Escherichia coli* between water extracts and AgNPs

ANOVA						
Source of Variation	SS	df	MS	F	P-value	F crit
Between Groups	150.5208333	1	150.5208333	4.8522498	0.0521947	4.9646027
Within Groups	310.2083333	10	31.02083333			
Total	460.7291667	11				

5. Discussion

The green synthesis of nanoparticles is the most preferred form of nanoparticle synthesis as the consumption of energy in the techniques is reduced hence more cost-effective, and the absence of chemicals in the production processes removes the risk of toxicity and contamination.[37] Despite the use of both microorganisms and plants in green synthesis, the use of plant extracts is favoured over microorganisms as the use of microorganisms is more time-consuming due to the isolation and maintenance of cell cultures along with possibility of contamination.[50] Furthermore, the phytochemicals in the leaves act as reducing agents in the reduction of metal ions into nanoparticles.[51]

When selecting a solvent for leaf extraction, water over methanol or ethanol was selected as it is non-toxic, non-inflammable and removes the need for purification. In addition, the synthesized nanoparticles partially oxidize due to the presence of oxygen in water.[52]

The synthesis of nanoparticles can be affected by several external factors. When synthesizing the AgNPs from the leaf extracts of *Diospyros*, the factors of temperature and reaction time were adjusted to determine the optimum conditions for the reaction. The optimum conditions for the synthesized nanoparticles are at 90 °C for 1 hour. Whereas nanoparticles were synthesized at 60 °C and at room temperature, the increase in absorbance is greater when synthesized at 90 °C as higher temperatures result in the higher rate of formation of nanoparticles hence a greater concentration of nanoparticles leading to a higher absorbance.[53,54] However, nanoparticles formed at higher temperatures are of a smaller average size compared to nanoparticles synthesized at a lower temperature.[55]

The colour change from a light-yellowish solution to a dark reddish-brown solution, observed during the formation of nanoparticles is due to surface plasmon resonance (SPR).[56] SPR occurs when the plasmons on the surface of the nanoparticles are excited by the incident light at a specific wavelength, leading to a decrease up the intensity of the light reflected.[57,58] This decrease in reflected light causes the decrease in absorbance giving a "peak" in UV-Visible spectrum at the 420 nm wavelength, indicating the formation of AgNPs.[59] In order to characterize the nanoparticles synthesized, through TEM, the morphology of the S05 AgNPs was determined as spherical with an average diameter of 30 nm under a range of 20 – 40 nm. However, previous studies on *Diospyros montana* AgNPs of an irregular shape with an average diameter of 18 nm.[60]

Further optical properties of AgNPs were determined by calculating the band gap energy. The band gap energy can be defined as the minimum amount of energy required to excite an electron to jump from the valence band to the conduction band.[61,62]

If the bandgap energy is less than 3.0 eV, the nanoparticles are classified as semiconductors whereas if the bandgap energy is more than 4.0 eV, the nanoparticles are classified as insulators.[63] The bandgap energies were calculated using the Planck's equation given below (Figure 26).

$$E = h \times \frac{C}{\lambda}$$

$$1\ eV = 1.6022 \times 10^{-19}\ J$$

E – Bandgap Energy (J)

h – Planck's constant (6.626×10^{-34} J s

C – Speed of Light (6.626×10^{8} m s^{-1})

λ – Peak Wavelength of AgNP

Figure 26. Planck's equation

Table 12 shows the bandgap energies of the nanoparticles calculated to be less than 3.0 eV, classifying them as semiconductors.

Table 12. Classification of AgNPs based on bandgap energy

Sample	Bandgap Energy		Classification
	Joules	eV	
Diospyros affinis	4.73×10^{-19}	2.96	
Diospyros atrata	4.73×10^{-19}	2.96	
Diospyros ebenum	4.79×10^{-19}	2.99	Semiconductor
Diospyros oocarpa	4.73×10^{-19}	2.96	
Diospyros quaesita	4.52×10^{-19}	2.82	

Despite limited research on *Diospyros* AgNPs, the nanoparticles along with the water extracts were subjected to antioxidant assays to determine and compare their antioxidant capabilities.

Flavonoids are a class of polyphenolic derivatives containing at least one hydroxyl group in the aromatic ring which acts as an electron donor, providing an antioxidant effect[64]. The TFC assay was carried out to quantify the content of flavonoids in the samples through an AlCl3 colourimetric assay at a maximum absorption wavelength of 415 nm, where AlCl3 binds to the C4 keto-group and the C3/C5 hydroxyl-group in flavonoids, forming an acid stable complex (Figure 27).[65, 66]
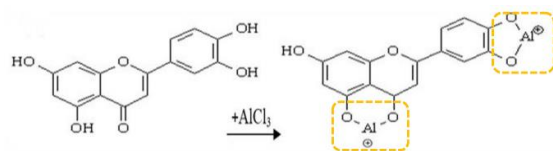
Figure 27. Formation of a flavonoid complex.[66]

The TFC of the AgNPs are significantly higher than the water extracts which can be seen in studies involving *Syzygium cumini* fruit extract due to the coating of flavonoids on the AgNPs.[67] The ANOVA test determined that there is a significant difference between the TFCs of the water extracts and AgNPs as the calculated P-value < 0.05 (0.008595), with S05 and S01 giving the highest and lowest TFCs respectively.

The TPC assay was carried out to quantify the content of phenols in the samples through a Folin-Ciocalteu colourimetric assay at a maximum absorption wavelength of 760 nm, where the Folin-Ciocalteu reagent is reduced by phenolic compounds to blue complexes (Figure 28).[68,69]
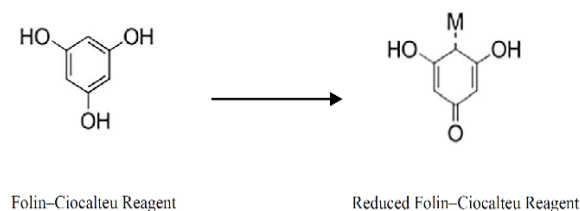
Figure 28. Reduction of Folin–Ciocalteu reagent.[69]

The TPC of the AgNPs are significantly greater than of the water extracts due to the accumulation of phenols by AgNPs (70). The ANOVA test determined that there is a significant difference between the TPCs of the water extracts and AgNPs as the calculated P-value < 0.05 (1.82×10^{-7}) with S05 and S01 giving the highest and lowest TPCs respectively.

The TAC of the samples was determined through the phosphomolybdenum assay at a maximum absorption wavelength of 695 nm where phosphate-molybdenum VI is reduced to phosphate-molybdenum V in the presence of antioxidants forming a green complex (Figure 29).[71-73]

The TACs of the AgNPs are significantly higher than the TACs of the water extracts indicating that the AgNPs have a higher abili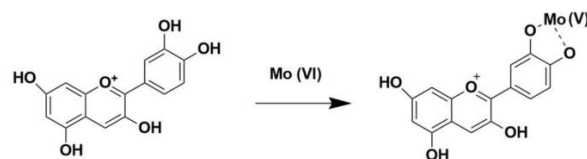ty to stabilize free-radicals which correlates with the high content of flavonoids and phenols.[74] The ANOVA test determined that there is a significant difference between the TACs of the water extracts and AgNPs as the calculated P-value (0.001638) is less than 0.05.

Figure 29. Reduction of Phosphate Molybdate VI.[73]

The DPPH radical scavenging assay was carried out to determine the antioxidant capabilities of the AgNPs by using a stable DPPH free radical which receives an electron from the antioxidants, stabilizing the molecules resulting in the discolouration of the violet DPPH solution.[75] The AgNPs have a greater % DPPH scavenging activity compared to the water extracts (Figure 15).

In addition to the DPPH assay, the IC_{50} of the samples was calculated to estimate the concentration of the sample required to stabilize 50% of the DPPH radicals where majority of the water extracts gave a higher IC_{50} compared to the AgNPs with the exception of S05 and S02 (Table 9).[76]

The IC_{50} values are inversely proportional to the antioxidant activity of the samples as a high IC_{50} indicates a high concentration is required to stabilize 50% of the DPPH radicals, concluding that the S02 and S05 AgNPs have greater antioxidant activities compared to the water extracts.[77]

The correlation between the antioxidant assays were analyzed and it was determined that a strong correlation existed between the assays (Figure 30). The TFC and TPC in the samples directly correlated with the calculated TAC indicating that content of flavonoids and phenols play a vital role in the TAC.
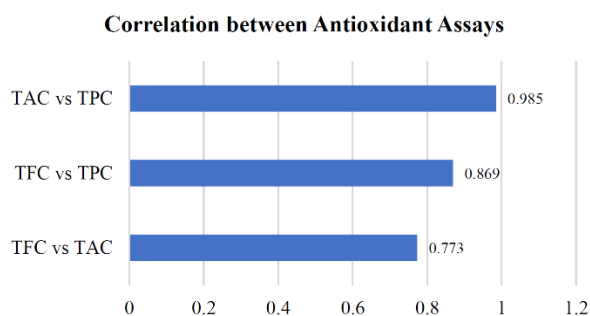
Figure 30. Correlation between antioxidant assays

The photocatalytic activity of the nanoparticles was compared by measuring the degradation of Eriochrome Black T (EBT) dye into intermediates where the N=N bond is dissolved (Figure 31) by free radicals formed by photocatalysis, resulting in a colourless solution.[78]
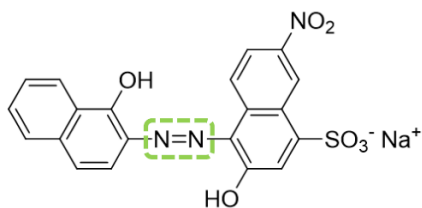
Figure 31. Chemical structure of Eriochrome Black T.[79]

The rate constant was calculated by using an ascorbic acid standard graph to calculate the concentrations at a given time and by following the below equation (Figure 32).

$$\text{Rate Constant} = \frac{\ln(\frac{C_t}{C_o})}{t}$$

C_o – Initial concentration

C_t – Peak concentration

t – Reaction time at peak concentration

Figure 32. Rate constant equation

The photocatalytic-degradation of EBT was carried out using S05 AgNPs of concentrations, 333 ppm and 5000 ppm, with and without NaBH$_4$ catalyst for a duration of 4 hours, in which the catalyzed reaction using 333 ppm AgNPs gave the highest degradation rate constant of 0.0271 (Figure 33 and Figure 34).

The addition of NaBH$_4$ significantly increases the degradation rate of the 333 ppm AgNPs from 0.0025 to 0.0271 as electrons from NaBH$_4$ are transferred to the EBT molecule by AgNPs, but the rate decreased as the AgNP concentration increased from 333 ppm to 5000 ppm possibly due to the formation of intermediates and the accumulation of excess AgNPs which cause excessive scattering of light, decreasing photocatalysis.[80-82]

A blue shift of the control peak can be seen in the graphs of the catalyzed photo-degradation of EBT (Figure 23 and Figure 25) which is caused by the formation of intermediates in the solution.[83]

When comparing the antibacterial activity, Figure 27 and Figure 28 reveals that the AgNPs have a greater antibacterial activity against *Staphylococcus aureus* and *Escherichia coli* as the AgNPs have higher zones of inhibition (ZOI) due to the action of the Ag$^+$ ions (Figure 03) where S05 had the highest ZOI against *Staphylococcus aureus* with S01 against *Escherichia coli* (84). AgNPs employ Ag$^+$ ions to exert bactericidal activity through the proposed mechanisms in Figure 3.

(A)

(B)
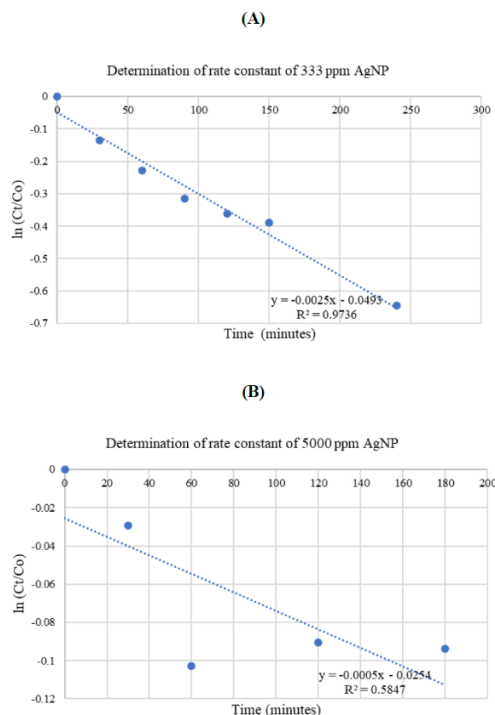
Figure 33. Rate constant graph of uncatalyzed AgNPs
(A – 333 ppm, B – 5000 ppm)

(A)

(B)
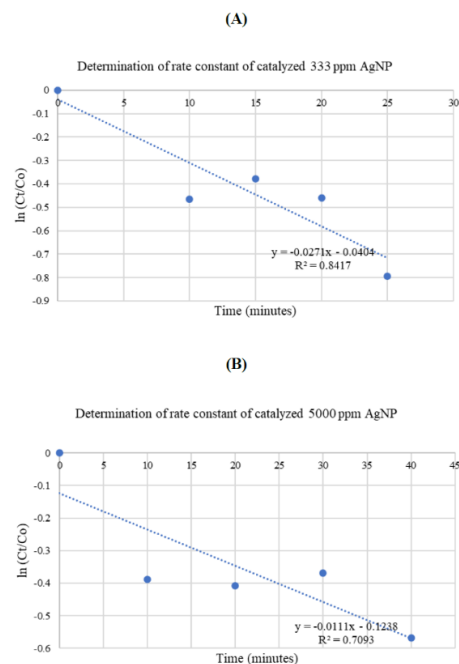
Figure 34. Rate constant graph of catalyzed AgNPs
(A – 333 ppm, B – 5000 ppm)

However, when comparing the ZOI of the AgNPs, the ZOI against *Escherichia coli* are greater than the ZOI of *Staphylococcus aureus.* Similar results were obtained in studies on SnO_2 nanoparticles concluded that the difference in antimicrobial activity was due to differences in the cell wall structure where *Escherichia coli* consists of a thin peptidoglycan layer containing lipopolysaccharides and proteins allowing easy entry for Ag^+ ions and less resistance to ROS compared to *Staphylococcus aureus.*[85, 86]

The P-values calculated for the ANOVA tests stated that there is a significant difference between the antibacterial activity against *Staphylococcus aureus* between the water extracts and AgNPs ($P<0.05$, $P=0.000511$), whereas there is no significant difference between the antibacterial activity against *Escherichia coli* of the water extracts and AgNPs ($P>0.05$, $P=0.052195$). However, the P-value calculated to determine a significant difference between the antibacterial activity between *Staphylococcus aureus* and *Escherichia coli,* was greater than 0.05 ($P= 0.617294$), concluding there is no significant difference.

Conclusion

AgNPs were synthesized using the six species of *Diospyros* with the exception of *Diospyros malabarica* at the temperatures of 25 °C, 60 °C and 90 °C for a time periods between 30 minutes to 72 hours where the optimum temperature was 90 °C. The phytochemical analysis on the water extracts confirmed that the leaves contained carbohydrates, proteins, saponins and terpenoids. TEM analysis determined that the synthesized AgNPs were spherical in shape with an average diameter of 30 nm. The AgNPs were subjected to antioxidant assays which determined that the AgNPs had a higher antioxidant capacity than the water extracts. The photocatalytic assays concluded that the 333 ppm AgNPs showed a higher photocatalytic activity when using $NaBH_4$. The antibacterial assays determined that the AgNPs show greater antibacterial activity against the bacterial strains where the activity against *Staphylococcus aureus* was greater than *Escherichia coli* due to structural differences in the cell wall. The determination of the following properties of the AgNPs allows for further studies and analysis for its implementation of its use into industries.

Acknowledgements

1. S. Bayda, M. Adeel, T. Tuccinardi, M. Cordani, and F. Rizzolio. *Molecules*, 2019;**25;**112.
2. GA. Silva. *Surgical Neurology*. 2004,**61**,216–220.
3. A. Zottel, A.V. Paska, and I. Jovčevska. *Diagnosis and Therapy Materials*, 2019,12.
4. A.K. Barui, R. Kotcherlakota, and C.R. Patra. *Metal Nanoparticles*, 2017;67-119.
5. A. Schröfel, G. Kratošovác, I. Šafaříka, M. Šafaříkováa, I. Raškae, and L.M. Shor. *Acta Biomaterialia*, 2014;**10**;4023-4042.
6. S.A. Polash, M. Hossain, T. Saha, and S. Sarker. *Emerging Trends in Nanomedicine*, 2021;81–127.
7. G. Pal, P. Rai, and A. Pandey. *Green Synthesis, Characterization and Applications of Nanoparticles*, 2019;1-26.
8. Z. Liu, L. Qi, X. An, C. Liu, and Y. Hu. *ACS Applied Materials and Interfaces*, 2017;**9**;40987–40997.
9. E.C. Wang, and A.Z. Wang. *Integrative Biology*, 2013; **6**;9-26.
10. K. Singh, A. Mishra, D. Sharma, and K. Singh. *Micro and Nano Technologies*, 2019;343-356.
11. C. Losasso, S. Belluco, V. Cibin, P. Zavagnin, I. Micetic, F. Gallocchio, M. Zanella, L. Bregoli, G. Biancotto, and A. Ricci. *Frontiers in Microbiology*. 2014;**5**;227.
12. Yin, J. Zhang, I.S. Zhao, M.L. Mei, Q. Li and C.H. Chu. *International Journal of Nanomedicine,* 2020;**15**;2555-2562.
13. S. Marimuthu, AJ. Antonisamy, S. Malayandi, K. Rajendran, PC. Tsai, A. Pugazhendhi, and VK. Ponnusamy. *Journal of Photochemistry and Photobiology B: Biology*. 2020;**205**;111823.
14. H. Nabika and K. Unoura. *Surface Chemistry of Nanobiomaterials*. 2016;**3**;231-263.
15. L. Wei, J. Lu, H. Xu, A. Patel, Z.S. Chen, and G. Chen. *Drug Discovery Today*. 2015;**20**;595-601.
16. J.K. Willcox, S.L. Ash, and G.L. Catignani. *Critical Reviews in Food Science and Nutrition*. 2004;**44**;275-295.
17. V. Goodarzi, H. Zamani, L. Bajuli, and A. Moradshahi. *Molecular Biology Research Communications*, 2014; **3**;165-174.
18. A. Flavia, and S. Addor. *The Science of the Antioxidant*, 2017;**92**;356-362
19. A. Phaniendra, D.B. Jestadi, and L. Periyasamy. *Indian Journal of Clinical Biochemistry*,2014;**30**;11-26.
20. D.J. Betteridge. *Metabolism*. 2000;**49**;3-8.
21. L.E. Cassagnes. *Research Gate*. 2015,10-15.
22. D. Gospodaryov, and V. Lushchak. *Oxidative Stress and Diseases*. 2012.
23. A. Yadav, R. Kumari, A. Yadav, JP. Mishra, S. Srivastava, and S. Prabha. *Research in Environment and Life Science*, 2016;**9**;1328-1331.
24. U. Nagaich, N. Gulati, and S. Chauha. *Journal of Pharmaceutics*, 2016;1-8.
25. E.M. Modan and A.G. Plăiaşu. *Metallurgy and Materials Science*, 2020;**43**;53-60.
26. X. Fu, J. Cai, X. Zhang, W-D. Li, H. Ge, and Y. Hu. *Advanced Drug Delivery Reviews*, 2018;**132**;169-187.
27. J.K. Patra, and K-H. Baek. *Journal of Nanomaterials*, 2014;1-12.
28. F.A. Khan. *Applications of Nanomaterials in Human Health*, 2020;15-21.
29. S. Kumar, P. Bhushan, and S. Bhattacharya. *Environmental, Chemical and Medical Sensors*, 2017;167-198.
30. S. Iravani, H. Korbekandi, SV. Mirmohammadi, and B. Zolfaghari. *Research in Pharmaceutical Sciences*, 2014;**9**;385–406.

31. D. Titus, E.J.J. Samuel, and S.M. Roopan. *Green Synthesis, Characterization and Applications of Nanoparticles*, 2019;303-319.

32. S.S. Salem, and A. Fouda. *Biological Trace Element Research*, 2020;**199**;344-370.

33. A. Roy, O. Bulut, S. Some, A.K. Mandal, and MD. Yilmaz. *RSC Advances*, 2019;**9**;2673–2702.

34. S. Ponarulselvam , C. Panneerselvam, K. Murugan, N. Aarthi, K. Kalimuthu, and S. Thangamani. *Asian Pacific Journal of Tropical Biomedicine*, 2012;**2**;574-580.

35. N. Phougat, M. Kumar, R.V. Saini, and A.K. Chhillar. *Metabolic Engineering for Bioactive Compounds,* 2017;**2**;49-268.

36. P. Kuppusamy, M.M. Yusoff, G.P. Maniam, and N. Govindan. *Saudi Pharmaceutical Journal,* 2016;**24**;473-484.

37. K. Parveen, V. Banse, and L. Ledwani. *AIP Conference Proceedings,* 2016;**1724**;020048.

38. P. Rauwel, S. Küünal, S. Ferdov, and E. Rauwel. *Advances in Materials Science and Engineering,* 2015;1-9.

39. K.K. Bharadwaj, B. Rabha, S. Pati, B.K. Choudhury, T. Sarkar, SK. Gogoi, N. Kakati, D. Basihya, ZA. Kari, and HA. Edinur. *Nanomaterials*, 2021;**11**;1999

40. A. Rauf, G. Uddin, S. Patel, A. Khan, SA. Halim, S. Bawazeer, K. Ahmad, N. Muhammed, and M.S. Mubarak. *Biomedicine and Pharmacotherapy,* 2017;**91**;714-730.

41. C. Xie, Z. Xie, X. Xu, and D. Yang. *Journal of Ethnopharmacology*, 2015;**163**;229-240.

42. V.S.S. Kantamreddi, and C.W. Wright. *Evidence-Based Complementary and Alternative Medicine*, 2018;**5**;187-190.

43. L. Valgimigli, A. Baschieri, and R. Amorat. *Journal of Materials Chemistry B*, 2018;**6**;2036-2051.

44. K. Kokila, N. Elavarasan, and V. Sujatha. N*ew Journal of Chemistry*, 2017;**41**;7481-7490.

45. S. Hamedi, and S.A. Shojaosadati. *Polyhedron.* 2019;**171**;172-180.

46. BN. Esfahani, F. Hozoorbakhsh, K.H. Rashed, SA. Havaei, K. Heidari, and SH. Moghim. *Research in Pharmaceutical Sciences*, 2014;**9**;193–198.

47. M. Kandiah, and K.N. Chandrasekaran. *Journal of Nanotechnology*, 2021;1–18.

48. Y. Baravaliya, M. Kaneria, Y. Vaghasiya, J. Parekh, and S. Chanda. *Turkish Journal of Biology*, 2009;**33;**159-164.

49. A.B. Aliyu, MA. Ibrahim, A.M. Musa, A.O. Musa, JJ. Kiplimo, and OA. Oyewale. *Acta Poloniae Pharmaceutica*, 2013;**70**;115-121.

50. M. Mohammadlou, H. Maghsoudi, and H. Jafarizadeh-Malmiri. *International Food Research Journal*, 2016;**23**;446-463.

51. J. Singh, T. Dutta, K-H. Kim, M. Rawat M, P. Samddar, and P. Kumar. *Journal of Nano biotechnology*, 2018;**16**;84.

52. H. Duan, D. Wang, and Y. Li. *Chemical Society Reviews*, 2015;**44**;5778-5792.

53. C.P. Devatha, and A.K. Thalla. *Synthesis of Inorganic Nanomaterials*, 2018;169-184.

54. M. Shah, D. Fawcett, S. Sharma, S. Tripathy, and G. Poinern. *Materials*, 2015;**8**;7278-7308.

55. HM. Kredy. *Semantic Scholar*, 2018.

56. M. Vanaja, K. Paulkumar, G. Gnanajobitha, S. Rajeshkumar, C. Malarkodi, and G. Annadurai. *International Journal of Metals*, 2014;1-8

57. A. Loiseau, V. Asila, G. Boitel-Aullen, M. Lam, M. Salmain, and S. Boujday. *Biosensors*, 2019;**9**;78.

58. Y. Tang, X. Zeng, and J. Liang. *Journal of Chemical Education*, 2010;**87**;742-746.

59. H. Kaur, and A. Sharma. *Materials Today: Proceedings,* 2021;**37;**3574-3576.

60. K.S. Siddiqi, M. Rashid, Tajuddin, A. Husen, and S. Rehman. *BioNanoScience,* 2019;**9**;302-312.

61. P. Makuła, M. Pacia, and W. Macyk. *The Journal of Physical Chemistry Letters*, 2018;**9**;6814-6817.

62. O.A. Jianu, G.F. Naterer, and M.A. Rosen. *Handbook of Generation IV Nuclear Reactors*, 2016;637-659.

63. D. Sundeep, T.V. Kumar, P.S.S. Rao, R.N. Ravikumar, and A. Gopala-Krishna. *Progress in Biomaterials*, 2017;**6**;57-66.

64. S. Aryal, M.K. Baniya, K. Danekhu, P. Kunwar, R. Gurung, and N. Koirala. *Plants,* 2018;**8**;96.

65. A. Win, A.M.T. Nyo, and K.M. Lwin. *International Journal of Scientific and Research Publications,* 2019;**9**;89101

66. S. Sepahpour, J. Selamat, M.A. Manap, A. Khatib, and AA. Razis. *Molecules*, 2018;**23**;402.

67. A.K. Mittal, J. Bhaumik, S. Kumar, and U.C. Banerjee. *Journal of Colloid and Interface Science*, 2014;**415**;39-47.

68. M. Tapera, S.A. Gitore, T. Shumba, N.P. Male, and S. Kaseke. *International Journal of Advance Study and Research Work*, 2019;**2**(2);2581-599.

69. L. Ford, K. Theodoridou, G.N. Sheldrake, and PJ. Walsh. *Phytochemical Analysis*, 2019;**30;**587-599.

70. Z. Bedlovičová, I. Strapáč, M. Baláž, and A. Salayová. *Molecules,* 2020;**25**;3191.

71. HF. Maswada. *Journal of Medical Sciences*, 2013;**13**;546-554.

72. R.A. Khan, M.R. Khan, S. Sahreen, and M. Ahmed. *Chemistry Central Journal*, 2012;**6**(1);43

73. J. Fowsiya and G. Madhumitha. *IOP Conference Series: Materials Science and Engineering*. 2017; **263**;022018.

74. M. Devi, B. Wibowotomo, S. Soekopitojo, and D. Merawati. *Proceedings of the 2nd International Conference on Vocational Education and Training*. 2019;**242**;7.

75. S.B. Kedare, and R.P Singh. *Journal of Food Science and Technology*. 2011;**48**,412-422.

76. B.S. Hendriks. *Current Opinion in Chemical Biology*. 2010;**14**;489-497.

77. M. Yunus, E. Suprihati, and A. Wijaya. *Systematic Reviews in Pharmacy*, 2021;**12**;1261-1266.

78. A. Ajmal, I. Majeed, R.N. Malik, H. Idriss, and MA. Nadeem. *RSC Advances*, 2014;**4**;37003-37026.

79. L.S. Omer, and R.J. Ali. *International Journal of Chemistry*, 2017;**9**;49.

80. D. Gola, A. Kriti, N. Bhatt, M. Bajpai, A. Singh, A. Arya, N. Chauhan, S.K. Srivastava, P.K. Tyagi, and Y. Agrawal. *Current Research in Green and Sustainable Chemistry*, 2021;**4**;100132.

81. A. Rafiq, M. Ikram, S. Ali, F. Niaz, M. Khan, Q. Khan, and M. Maqbool. *Journal of Industrial and Engineering Chemistry*, 2021;**97**;111-128.

82. KM. Reza, A. Kurny, and F. Gulshan. *Applied Water Science*. 2015;**7**;1569-1578.

83. Z. Othman, A. Sinopoli, HR. Mackey and KA. Mahmoud. *ACS Omega*, 2021;**6;**33325-33338.

84. I.X. Yin, J. Zhang, IS. Zhao, ML. Mei, Q. Li, and C.H. Chu. *International Journal of Nanomedicine*, 2020;**15**;2555-2562.

85. J. Gouyau, RE. Duval, A. Boudier, and E. Lamouroux. *International Journal of Molecular Sciences*, 2021,**22**,1905.

86. S.M. Amininezhad, A. Rezvani, M. Amouheidari, S. Amininejad and S. Rakhshani. *Zahedan Journal of Research in Medical Sciences*, 2015;**17**(9); e1053.